iScience

CellPress
OPEN ACCESS

Article

The association of appendectomy with prognosis and tumor-associated macrophages in patients with colorectal cancer

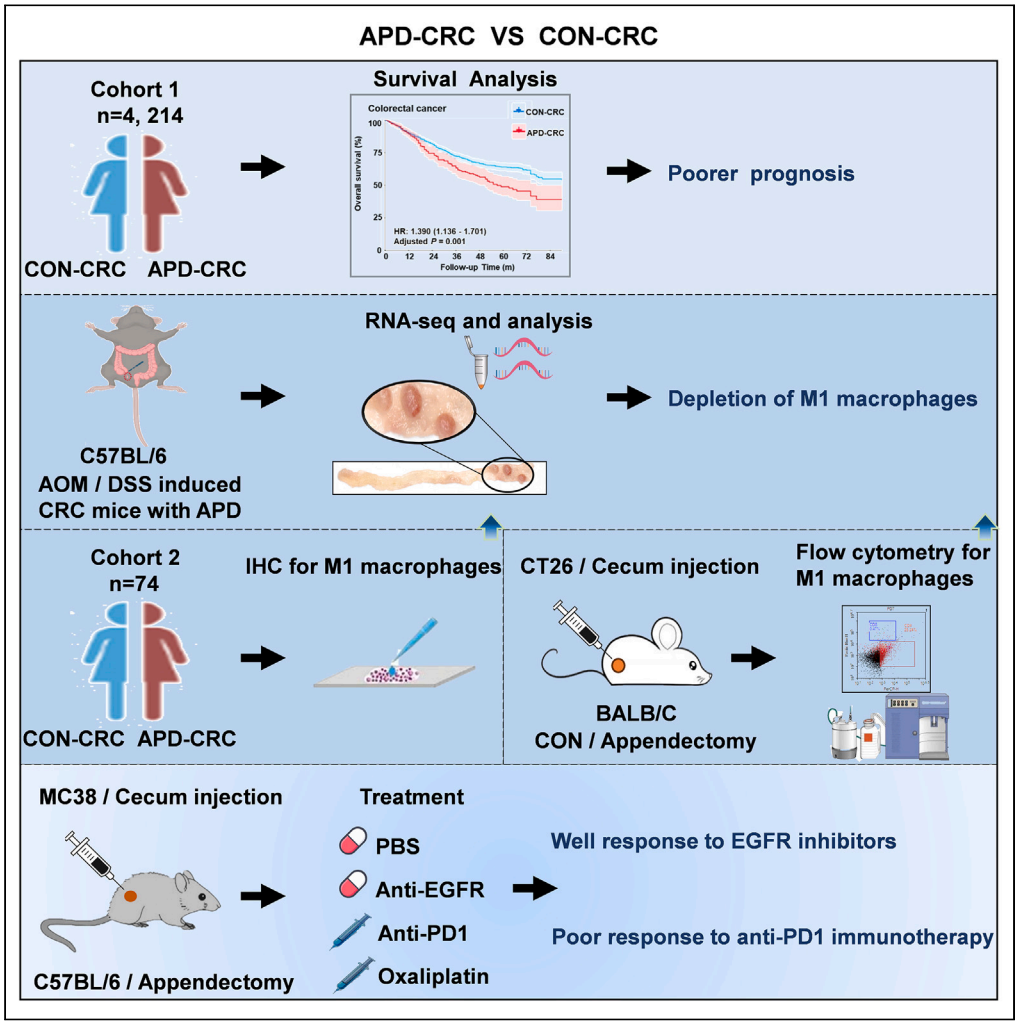

Gaixia Liu, Chenhao Hu, Jiangpeng Wei, ..., Gang Ji, Junjun She, Feiyu Shi

shejunjun@xjtu.edu.cn (J.S.)
011357@xjtufh.edu.cn (F.S.)

Highlights

Losing normal function of the appendix is a prognostic biomarker for CRC

Depletion of M1 macrophages in APD-CRC confers impaired survival

APD-CRC are well response to EGFR inhibitors and poor response to immunotherapy

Liu et al., iScience 27, 110578
September 20, 2024
https://doi.org/10.1016/j.isci.2024.110578

iScience

CellPress
OPEN ACCESS

Article

The association of appendectomy with prognosis and tumor-associated macrophages in patients with colorectal cancer

Gaixia Liu,[1,2,3,5] Chenhao Hu,[1,2,3,5] Jiangpeng Wei,[4] Qixin Li,[1,2,3] Jiaqi Zhang,[2,3] Zhe Zhang,[1,2,3] Penghong Qu,[1,2,3] Zeyu Cao,[1,2,3] Ruochen Wang,[2,3] Gang Ji,[4] Junjun She,[1,2,3,*] and Feiyu Shi[1,2,3,6,*]

SUMMARY

The vermiform appendix plays an important role in colorectal immunity and the homeostasis of the gut microbiome. We aimed to evaluate the prognostic value of prior appendectomy for patients with colorectal cancer (CRC). This study revealed that prior appendectomy is an independent risk factor for the prognosis of patients with CRC, based on a multicentral CRC cohort. We further demonstrated that appendectomy induced a poor prognosis of CRC through the depletion of M1 macrophage cells in AOM-induced mice, which was confirmed in age-, sex-, and location-matched patients' cohorts and orthotopic model models with the CT26 cell line. Poor responses to anti-PD-1 immunotherapy were detected in patients with CRC with appendectomy, and cetuximab is an effective treatment for patients with appendectomy-associated colorectal cancer (APD-CRC) to improve their prognosis. Our study will provide a reference for developing treatment plans for a considerable number of patients with APD-CRC, which is of great clinical significance.

INTRODUCTION

CRC is one of the most common digestive malignancies, with almost 1,800,000 new cases in the world each year and CRC annually results in nearly 900,000 cancer-related deaths worldwide.[1] As such, efforts to identify the risk factors contributing to the prognosis of CRC are increasingly important not only in clinical treatment but also in public health.

Appendectomy is one of the most common abdominal operations, with the clinical application of more than a century.[2] According to recent studies on the appendix, its primary function includes acting as an auxiliary lymphoid organ in detecting and eliminating pathogens, as well as functioning as a "Bacterial Safe House" to protect and regulate gut commensal microbiota.[3] Given the important roles of gut immune state and gut microbiota in CRC, appendectomy is believed to be closely related to CRC.[3–5] Furthermore, some epidemiological studies and clinical observations also have indicated an intimate association between prior appendectomy and CRC, particularly in terms of the increased risk of subsequent development of CRC.[6–8] According to our previous study, appendectomy-induced microbial dysbiosis plays a crucial role in CRC development.[9] Nevertheless, as far as we know, few studies investigated the prognostic significance of prior appendectomy for patients with CRC, which was very important considering the high prevalence of appendectomy and its potential impact on treatment management and follow-up strategies.

Considering the role of the appendix as an important part of the intestinal immune system as well as the significant impact of tumor microenvironment (TME) on immunotherapy,[10] it is necessary to further evaluate the TME of CRC with appendectomy. Considerable evidence has indicated that a high-level gut local immune response is significantly associated with improved clinical outcomes in CRC. In particular, tumor-associated macrophages (TAMs) represent the most abundant innate immune population in the TME. TAMs influence cancer cell growth and metastasis and mediate immunosuppressive effects on the adaptive immune cells of the TME.[11] Furthermore, macrophages are highly plastic and often display an immune-suppressive M2-like phenotype that fosters tumor growth and promotes resistance to therapy. TAMs can also acquire an anti-tumorigenic M1-like phenotype and enhance the response to immunotherapy.[12]

To investigate the potential correlation between prior appendectomy and the prognosis influence on patients with CRC, we first conducted a multicenter prospective study involving 4,214 subjects to assess the relationship between appendectomy and CRC prognosis. In addition, we then used two CRC mouse models with appendectomy to investigate the mechanism behind appendectomy-induced poor

[1]Department of General Surgery, The First Affiliated Hospital of Xi'an Jiaotong University, Xi'an, Shaanxi, China
[2]Center for Gut Microbiome Research, Med-X Institute, The First Affiliated Hospital of Xi'an Jiaotong University, Xi'an, Shaanxi, China
[3]Department of High Talent, The First Affiliated Hospital of Xi'an Jiaotong University, Xi'an, Shaanxi, China
[4]Department of Digestive Surgery, Xijing Hospital, Air Force Military Medical University, Xi'an, China
[5]Senior author
[6]Lead contact
*Correspondence: shejunjun@xjtu.edu.cn (J.S.), 011357@xjtufh.edu.cn (F.S.)
https://doi.org/10.1016/j.isci.2024.110578

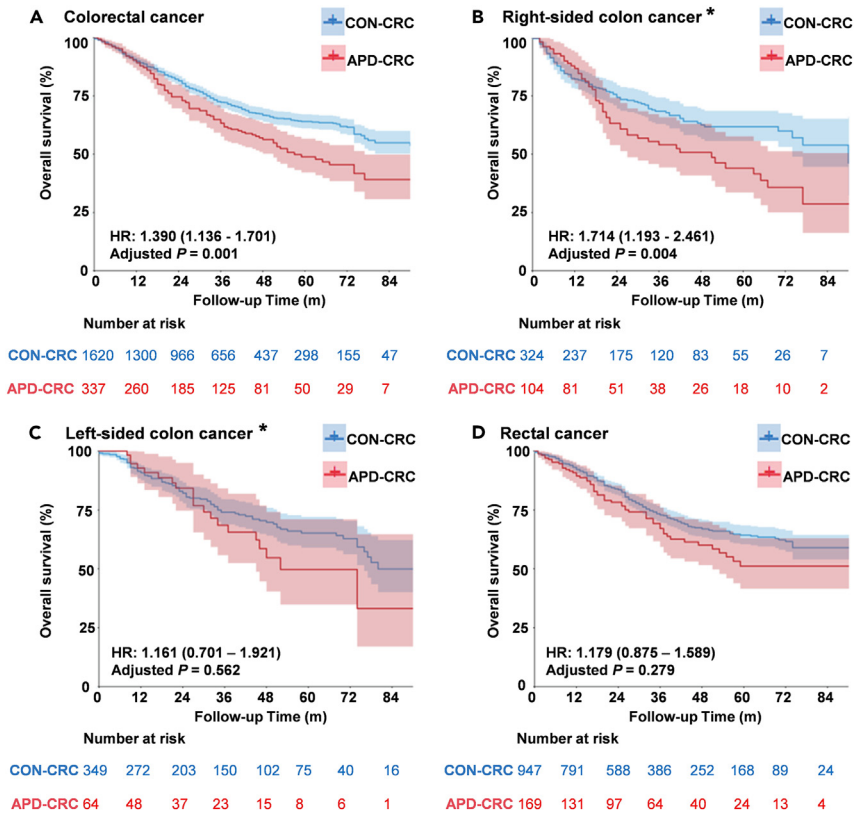

Figure 1. Patients with CRC with prior appendectomy had a worse overall survival than patients without appendectomy, especially with right-sided colon cancer

(A) Kaplan-Meier curves of overall survival for patients with CRC with and without prior appendectomy.

(B–D) Subgroup analysis was performed to evaluate the overall survival of right-sided colon cancer, left-sided colon cancer, and rectal cancer for patients with CRC with appendectomy. * Right-sided colon cancer includes cancer at the cecum, ascending colon, hepatic flexure, and transverse colon. Left-sided colon cancer includes cancer at the splenic flexure, descending colon, and sigmoid colon.

prognosis of CRC. Also, the curative effect of different chemotherapy regimens and immunotherapy for patients with CRC with prior appendectomy were evaluated.

RESULTS

Overall characteristics of cohorts

A total of 4,214 patients with CRC were included in the study, which included 342 patients with appendectomy history and 3,872 patients without appendectomy history (Figure S1). 337/342 patients with CRC with appendectomy were included in the propensity score analysis and matched 1:5 with CON-CRC (non-appendectomy). The baseline characteristics and distribution of propensity scores in the matched cohort were comparable between groups (Table S1). After matching, the median ages were 65 (58–73) and 65 (57–72) years in the appendectomy-CRC and CON -CRC groups. A total of 43.9% and 45.2% of patients were male in the appendectomy-CRC and CON -CRC groups.

Patients with colorectal cancer with prior appendectomy had worse survival than patients without appendectomy, especially the right-sided colon cancer

We calculated the OS and DFS for patients with CRC in our cohort by Kaplan-Meier survival analysis and multivariate Cox regression analysis. Confounding factors include sex, age, tumor stage, tumor differentiation, smoking, drink, CRC family history, Chemoradiotherapy, and CCI score. The results showed worse OS and DFS in patients with CRC with prior appendectomy (Figures 1 and 2; Tables 1 and 2). The HR of OS survival was 1.39 (1.136–1.701, Adjusted $p = 0.001$, Figure 1A; Table 1) and the HR of DFS survival was 1.813 (1.461–2.249, Adjusted $p < 0.001$, Figure 2A; Table 2). The result remained robust in the sensitivity analysis with different statistical modeling (Tables S2–S5). In subgroups analysis by tumor location, we observed more significantly decreased OS in patients with right-sided colon cancer with appendectomy [1.714 (1.193–2.461), Adjusted $p = 0.004$, Figure 1B and Table 1] than in control cases. And, there was no difference between patients with or without appendectomy for left-sided patients with colon cancer [1.161 (0.701–1.921), adjusted $p = 0.562$, Figure 1C and Table 1] and patients with

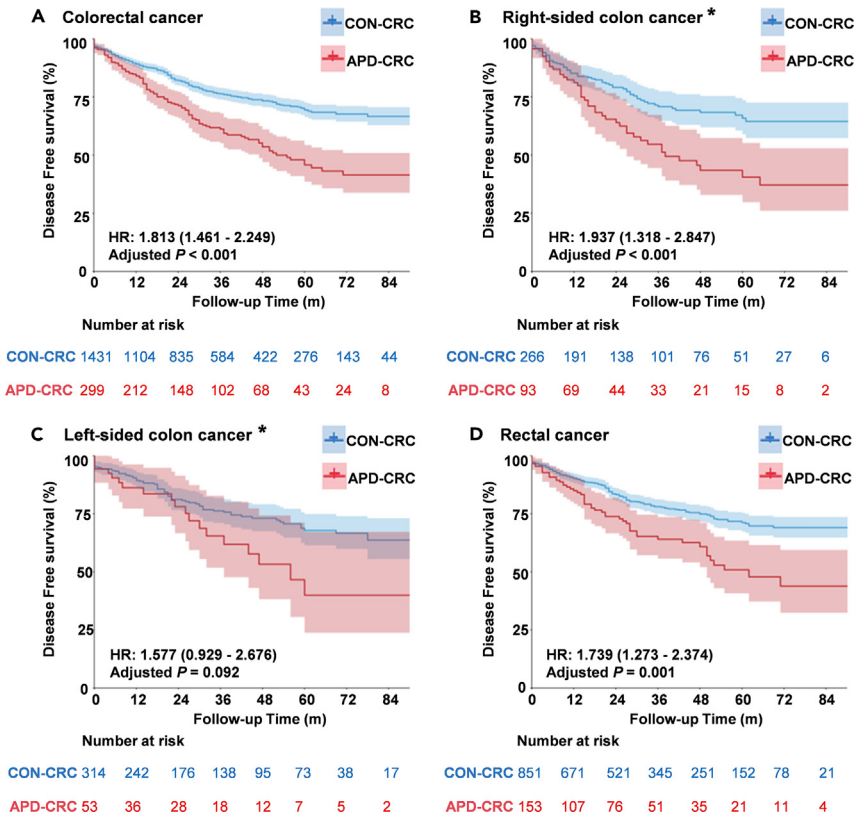

Figure 2. Patients with CRC with prior appendectomy had a poorer DFS than patients without appendectomy

(A) Kaplan-Meier curves of DFS for patients with CRC with and without prior appendectomy.

(B–D) Subgroup analysis was performed to evaluate DFS of right-sided colon cancer, left-sided colon cancer, and rectal cancer for patients with CRC with appendectomy. * Right-sided colon cancer includes cancer at the cecum, ascending colon, hepatic flexure, and transverse colon. Left-sided colon cancer includes cancer at the splenic flexure, descending colon, and sigmoid colon.

rectal cancer [1.179 (0.875–1.589), Adjusted $p = 0.279$, Figure 1D and Table 1]. But analysis for DFS showed that a significant and independent association between appendectomy and DFS remained in patients with right-sided colon cancer [1.813 (1.461–2.249), Adjusted $p < 0.0001$, Figure 2B and Table 2], and patients with rectal cancer [1.739 (1.273–2.374), Adjusted $p = 0.001$, Figure 2D and Table 2].

In subgroups analysis by tumor stage, more significantly decreased OS were overserved in patients with stageIandIIstage right-sided colon cancer with appendectomy compared with control cases [SHR: 1.973 (1.068–3.646), adjusted $p < 0.05$, Table S6]. Moreover, both patients with I/II and III stage CRC with appendectomy had poorer FDS than controls [stage I/II, SHR: 1.681 (1.209–2.336), Adjusted $p = 0.002$; stage III, SHR: 1.863 (1.398–2.482), adjusted $p < 0.001$, Table S7].

In conclusion, losing the function of the appendix (appendectomy) could be considered an independent prognostic risk factor for CRC, especially right-sided colon cancer.

Appendectomy-colorectal cancer with the alteration of immune microenvironment was characterized by the low density of M1 macrophages

To investigate the potential mechanisms behind the poor prognosis in patients with CRC with appendectomy, we utilized a CRC mouse model induced by the administration of AOM combined with DSS[13] (Figure 3A). We harvested colon tumor tissue from appendectomy ($n = 5$) and control mice ($n = 3$) for RNA sequencing at the end of the induction period. The data revealed that APD-CRC is distinct from CON-CRC, with 46 genes upregulated and 101 genes downregulated in the APD-CRC (Table S8). Genes involved in the negative regulation of lymphocyte activation, regulation of the immune system process, and innate immune response show significant differences between APD-CRC and CON-CRC (Figure S2). So, the proportion of infiltrating immune cells in tumor tissue was estimated, which revealed that the density of M1 macrophage was significantly depleted in APD-CRC compared with CON-CRC (Figure 3B). Histological examination of colon tumor sections confirmed that the appendectomy induced depletion of M1 macrophage in colon cancer as evidenced by significantly decreased CD80 positive and iNOS positive cells (Figure 3C).

We further validated the association between appendectomy and infiltration of M1 macrophage cells in patients with CRC. We compared densities of M1 macrophage in tumor tissue from 37 CRC cases with appendectomy and 37 age-, gender- and location-matched control CRC

Table 1. Multivariable COX regression analyses for association between prior appendectomy and OS of patients with CRC after PS matching

	Total colorectal cancer		Right-sided colon cancer[a]		Left-sided colon cancer[a]		Rectal cancer	
	SHR (95% CI)	Adjusted *P*	SHR (95% CI)	Adjusted *P*	SHR (95% CI)	Adjusted *P*	SHR (95% CI)	Adjusted *P*
Appendectomy, yes vs. no	1.39 (1.136–1.701)	0.001	1.714 (1.193–2.461)	0.004	1.161 (0.701–1.921)	0.562	1.179 (0.875–1.589)	0.279
Sex, male vs. female	0.962 (0.803–1.154)	0.678	1.185 (0.828–1.698)	0.354	1.556 (0.988–2.45)	0.056	0.76 (0.591–0.976)	0.032
Age, years	1.032 (1.024–1.041)	0	1.027 (1.011–1.044)	0.001	1.017 (0.997–1.038)	0.098	1.04 (1.028–1.052)	0
Stage, II vs. I	1.596 (1.067–2.388)	0.023	1.058 (0.376–2.981)	0.914	1.56 (0.557–4.369)	0.397	2.007 (1.221–3.298)	0.006
Stage, III vs. I	3.562 (2.417–5.249)	0	2.43 (0.863–6.839)	0.093	4.544 (1.702–12.136)	0.003	4.059 (2.523–6.532)	0
Stage, IV vs. I	10.015 (6.652–15.079)	<0.001	7.018 (2.47–19.94)	0	10.269 (3.761–28.04)	0	12.875 (7.686–21.565)	<0.001
Differentiation, moderate vs. low	0.707 (0.54–0.927)	0.012	1.092 (0.626–1.905)	0.757	0.92 (0.375–2.258)	0.856	0.483 (0.343–0.679)	0
Differentiation, high vs. low	1.315 (0.958–1.806)	0.091	2.328 (1.253–4.324)	0.007	1.913 (0.714–5.129)	0.197	0.794 (0.512–1.232)	0.304
Smoke, ex-smoker vs. none	0.958 (0.698–1.313)	0.788	0.849 (0.422–1.708)	0.647	1.749 (0.896–3.417)	0.102	0.735 (0.474–1.139)	0.168
Smoke, current vs. none	1.018 (0.766–1.352)	0.903	0.662 (0.346–1.267)	0.213	2.734 (1.349–5.539)	0.005	0.92 (0.629–1.346)	0.667
Drink, light vs. none	0.859 (0.568–1.298)	0.471	0.953 (0.32–2.839)	0.93	0.529 (0.178–1.575)	0.253	1.087 (0.644–1.837)	0.754
Drink, severe vs. none	0.451 (0.162–1.251)	0.126	0.363 (0.039–3.339)	0.37	0.885 (0.186–4.198)	0.877	0.323 (0.045–2.342)	0.263
CRC family history, family history of CRC vs. none	1.638 (1.135–2.365)	0.008	1.402 (0.673–2.922)	0.367	1.529 (0.724–3.227)	0.265	1.838 (1.057–3.197)	0.031
CRC family history, family history of other cancers vs. none	0.606 (0.348–1.053)	0.076	0.54 (0.212–1.377)	0.197	0.359 (0.087–1.473)	0.155	0.662 (0.292–1.502)	0.324
Chemoradiotherapy, yes vs. no	0.488 (0.407–0.587)	0	0.493 (0.341–0.713)	0	0.468 (0.305–0.717)	0	0.481 (0.373–0.62)	0
CCI score, 1 vs. 0	1.156 (0.967–1.383)	0.112	1.467 (1.023–2.103)	0.037	2.05 (1.386–3.031)	0	0.777 (0.6–1.005)	0.055
CCI score, ≥2 vs. 0	2.214 (1.425–3.44)	0	2.403 (1.09–5.299)	0.03	1.795 (0.399–8.078)	0.446	1.807 (0.995–3.283)	0.052

SHR: subdistribution hazard ratio; CI: confidence interval; CCI: Charlson comorbidity index; CRC: colorectal cancer.

[a]Right-sided colon cancer: cancer at cecum, ascending colon, hepatic flexure, and transverse colon. Left-sided colon cancer: cancer at splenic flexure, descending colon, and sigmoid colon.

Table 2. Multivariable COX regression analyses for association between prior appendectomy and DFS of patients with CRC after PS matching

	Total colorectal cancer		Right-sided colon cancer[a]		Left-sided colon cancer[a]		Rectal cancer	
	SHR (95% CI)	Adjusted *P*	SHR (95% CI)	Adjusted *P*	SHR (95% CI)	Adjusted *P*	SHR (95% CI)	Adjusted *P*
Appendectomy, yes vs. no	1.813 (1.461–2.249)	0	1.937 (1.318–2.847)	0.001	1.577 (0.929–2.676)	0.092	1.739 (1.273–2.374)	0.001
Sex, male vs. female	1.035 (0.84–1.276)	0.746	1.069 (0.705–1.62)	0.754	1.228 (0.764–1.973)	0.397	0.932 (0.698–1.243)	0.631
Age, years	1.021 (1.012–1.03)	0	1.01 (0.994–1.027)	0.213	1.01 (0.991–1.03)	0.31	1.032 (1.018–1.045)	0
Stage, II vs. I	2.07 (1.39–3.082)	0	2.103 (0.649–6.818)	0.216	1.036 (0.459–2.338)	0.932	2.664 (1.595–4.452)	0
Stage, III vs. I	3.437 (2.325–5.081)	0	3.503 (1.072–11.444)	0.038	1.868 (0.858–4.069)	0.116	4.175 (2.537–6.873)	0
Differentiation, moderate vs. low	0.682 (0.511–0.911)	0.009	1.132 (0.622–2.063)	0.685	0.443 (0.229–0.857)	0.016	0.578 (0.39–0.857)	0.006
Differentiation, high vs. low	1.099 (0.763–1.583)	0.613	2.271 (1.156–4.464)	0.017	0.579 (0.24–1.393)	0.222	0.842 (0.486–1.459)	0.54
Smoke, ex-smoker vs. none	0.941 (0.642–1.379)	0.755	1.127 (0.464–2.736)	0.792	1.134 (0.479–2.685)	0.775	0.823 (0.501–1.352)	0.442
Smoke, current vs. none	1.317 (0.971–1.788)	0.077	1.391 (0.749–2.583)	0.295	1.791 (0.871–3.682)	0.113	1.112 (0.739–1.674)	0.61
Drink, light vs. none	0.823 (0.513–1.32)	0.419	0.651 (0.221–1.916)	0.436	0.723 (0.189–2.772)	0.636	0.956 (0.53–1.722)	0.879
Drink, severe vs. none	0.9 (0.414–1.957)	0.791	1.282 (0.287–5.721)	0.745	0.443 (0.051–3.864)	0.461	0.878 (0.313–2.458)	0.804
CRC family history, family history of CRC vs. none	0.742 (0.439–1.257)	0.267	0.739 (0.29–1.883)	0.526	0.387 (0.092–1.635)	0.197	0.955 (0.461–1.976)	0.9
CRC family history, family history of other cancers vs. none	0.713 (0.398–1.276)	0.254	1.155 (0.415–3.215)	0.783	1.125 (0.306–4.133)	0.86	0.489 (0.198–1.209)	0.121
Chemoradiotherapy, yes vs. no	0.624 (0.508–0.766)	0	0.497 (0.323–0.765)	0.001	0.683 (0.437–1.066)	0.093	0.691 (0.523–0.914)	0.01
CCI score, 1 vs. 0	0.846 (0.683–1.047)	0.124	0.932 (0.61–1.424)	0.744	0.953 (0.595–1.526)	0.841	0.784 (0.582–1.056)	0.109
CCI score, ≥2 vs. 0	0.782 (0.322–1.9)	0.587	NA	0.994	1.525 (0.407–5.722)	0.531	0.483 (0.119–1.961)	0.309

SHR: subdistribution hazard ratio; CI: confidence interval; CCI: Charlson comorbidity index; CRC: colorectal cancer.
[a]Right-sided colon cancer: cancer at cecum, ascending colon, hepatic flexure, and transverse colon. Left-sided colon cancer: cancer at the splenic flexure, descending colon, and sigmoid colon.

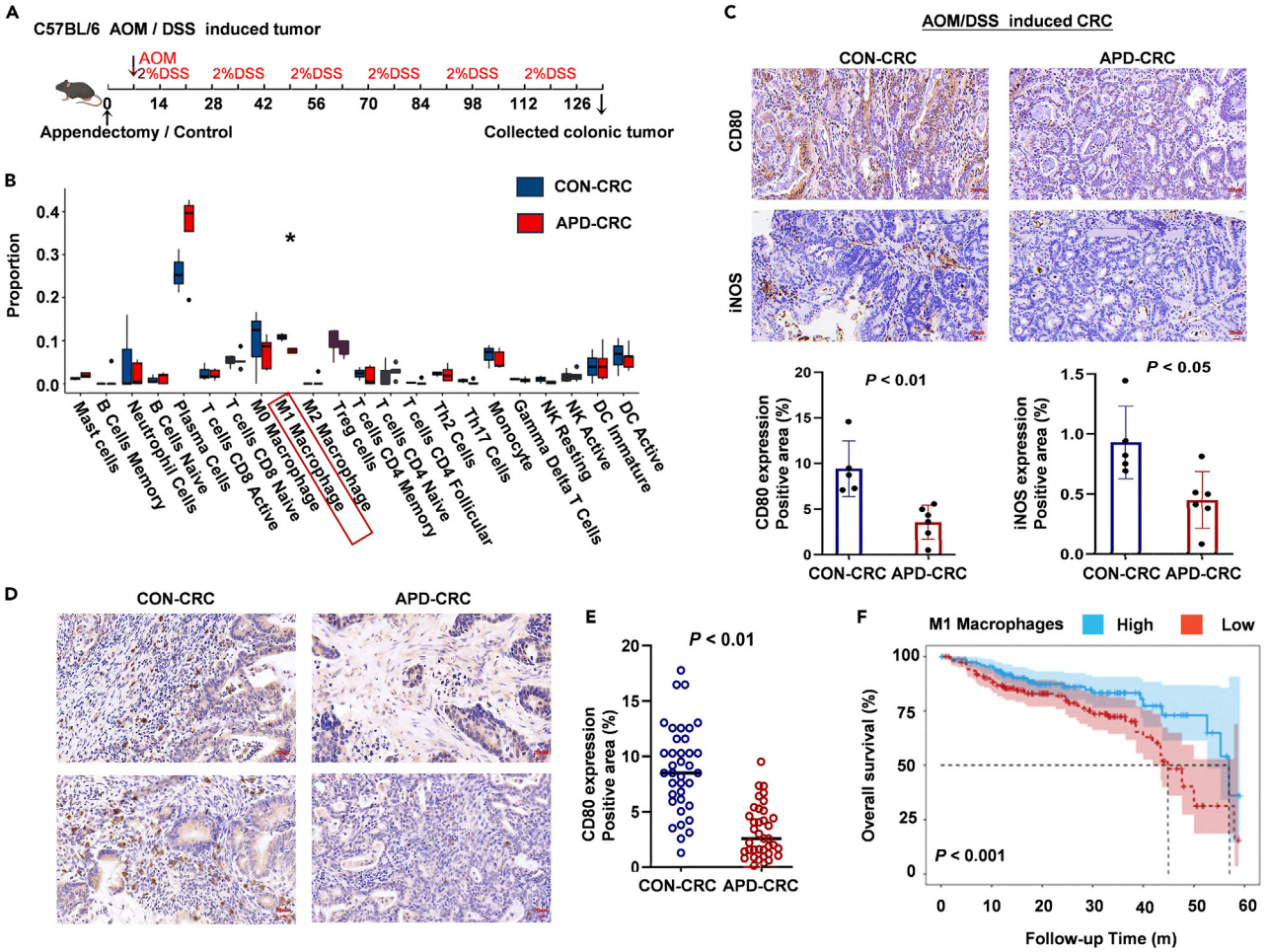

Figure 3. Appendectomy-CRC with the alteration of immune microenvironment was characterized by the low density of M1 macrophages

(A) The flow chart of the AOM induced colorectal cancer mouse with appendectomy model experiments.

(B) Bar plot shows the ratio differentiation of 22 types of immune cells between APD-CRC samples and CON-CRC samples from AOM induced CRC mice. *$p < 0.05$, **$p < 0.01$, Wilcoxon test.

(C) The CD80 and iNOS expression referring to the infiltration of M1 macrophages in CRC tissue from mice with (right, $n = 6$) and without (left, $n = 5$) appendectomy. Scale bar, 20um.

(D) Representative images of immunohistochemistry staining for CD80 for colorectal tumor species from patients with (right) or without (left) appendectomy. Scale bar, 20um.

(E) Quantitative analysis for the density of M1 macrophage in APD-CRC ($n = 37$) tissue and age-, sex- and location-matched CON-CRC ($n = 37$) tissue was presented.

(F) Kaplan-Meier survival analysis to assess the correlation between the density of M1 macrophage and OS outcome of patients with colorectum adenocarcinoma from TCGA database. Data are means ± SEM. The difference between the two groups was determined by a two-tailed Student's t test.

cases. The demographic and clinical characteristics of these participants are shown in Table S9. Indeed, colorectal carcinoma tissue from patients with appendectomy possesses a lower density of M1 macrophage compared with CRC tissue from controls (Figures 3D and 3E). Furthermore, the prognostic significance of M1 macrophage density was also validated in the TCGA CRC cohort (Figure 3F). Collectively, these results indicated that the feature of patients with CRC with appendectomy for immune microenvironment was lower density M1 macrophages.

Considering the complex relationship between the appendix, gut microbiota, and tumor immune microenvironment, we compared the abundance of two top CRC-promoting bacteria (Bacteroides vulgatus, Bacteroides fragilis) and beneficial bacteria (Blautia sp SC05B48, Collinsella aerofaciens) in tumor tissue from APD-CRC and CON-CRC, which we validated altered significantly in feces from case with appendectomy[9] (Figure S3A). The CRC cohort ($n = 35$. APD-CRC: CON-CRC = 1:2, matched by sex, age, location, and BMI) was established and the demographic and clinical characteristics of this cohort are shown in Table S10. The abundance of Blautia sp SC05B48, which is reported as a potential probiotic,[14] significantly decreased in cancer tissue from APD-CRC compared with CON-CRC (Figure S3A). Moreover, the connection between the density of M1 macrophages and the abundance of Blautia sp SC05B48 was validated in another CRC cohort through

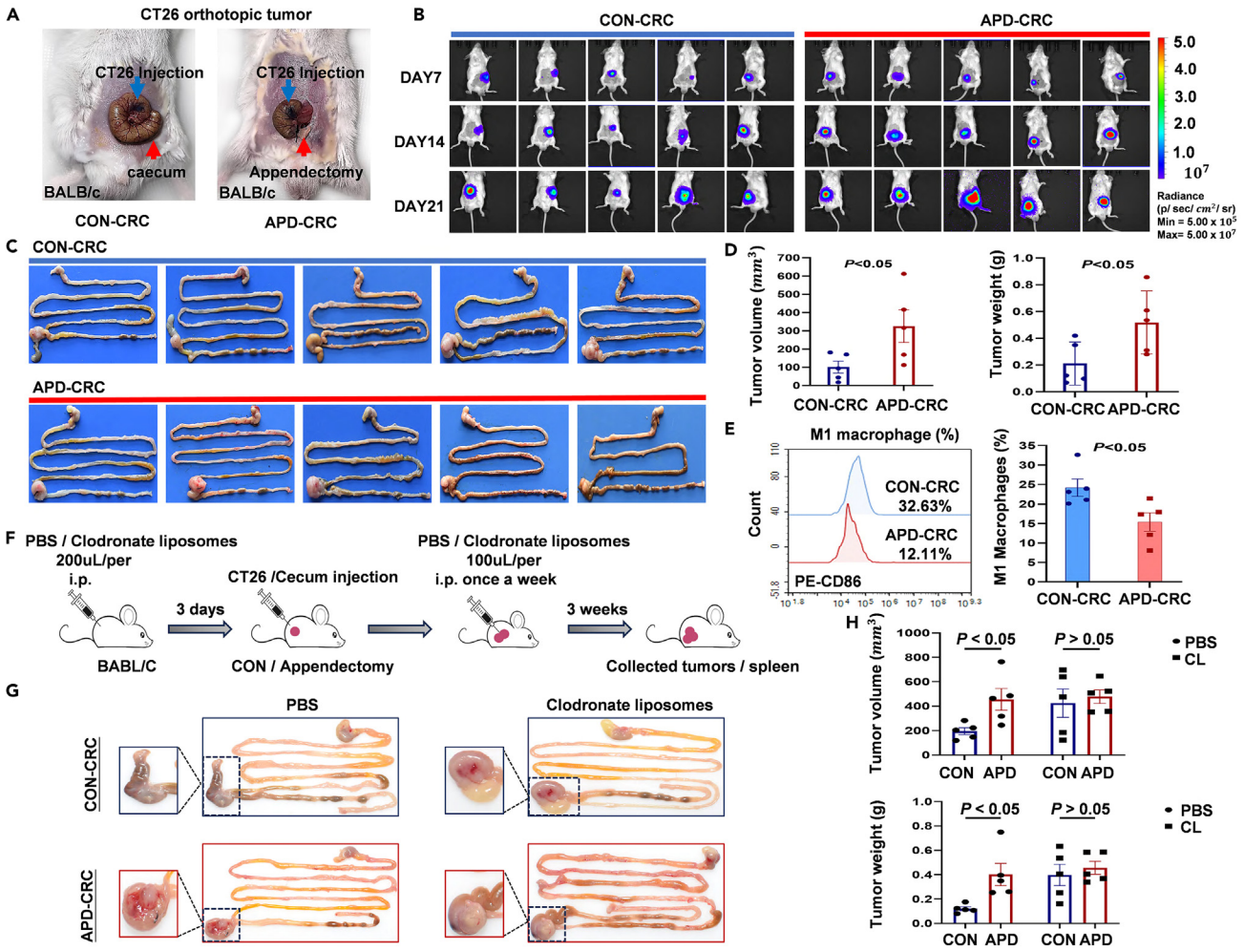

Figure 4. Depletion of M1 macrophage cells in cancer tissue contributes to a poor prognosis for CRC with appendectomy

(A) Representative pictures of CT26-luci cecum orthotopic mice with (APD-CRC) or without appendectomy (CON-CRC).

(B)The growth of orthotopic tumors in mice with appendectomy and controls was observed by a small animal live imaging instrument.

(C) Images for CT26-Luci cecum orthotopic tumors from mice with appendectomy and controls in the endpoint.

(D)Tumor volumes and tumor weights were compared between APD-CRC and CON-CRC.

(E) Frequencies of M1 macrophage cells in orthotopic tumors from ADP-mice (n = 5) and control-mice (n = 5) were measured by flow cytometry.

(F) The flow chart of clodronate liposomes inducing the depletion of macrophages in CT26-Luci cecum orthotopic tumors mice with/without appendectomy.

(G and H) Representative images of CT26-Luci cecum orthotopic tumors in CON-CRC and APD-CRC groups from mice treated by PBS/clodronate liposomes. Similar levels of tumor size and tumor weight were detected in macrophage-depleted mice with or without appendectomy. Data are means ± SEM. The difference between the two groups was determined by a two-tailed Student's t test.

RNA-seq and qPCR (n = 88, Table S11). CRC tissues with a high abundance of Blautia sp SC05B48 were characterized by enriched M1 macrophages (Figure S3B). Correspondingly, the data provides evidence for the reduction of M1 macrophages in CRC caused by appendectomy. The data suggested that appendectomy may play a key role in changing the density of M1 macrophages in APD-CRC by inducing intestinal bacteria dysbiosis.

Depletion of M1 macrophage cells in cancer tissue contributes to a poor prognosis for colorectal cancer with appendectomy

The influence of the depletion of M1 macrophages induced by appendectomy on the outcome of CRC was determined in orthotopic CRC mice. We generated CT26-Luci orthotopic tumor mice models with or without appendectomy (Figure 4A). Appendectomy mice demonstrated faster tumor growth observed by small animal live imaging instruments compared with control mice (Figure 4B). Appendectomy mice had increased tumor volume and tumor weight ($p < 0.05$, Figure 4C) compared with control mice at the endpoint (Figure 4D). Consistently, the flow Cytometry results showed that the proportion of infiltrating M1 macrophage cells was significantly decreased in CT26 orthotopic tumors from mice with appendectomy (Figures 4E and S4A).

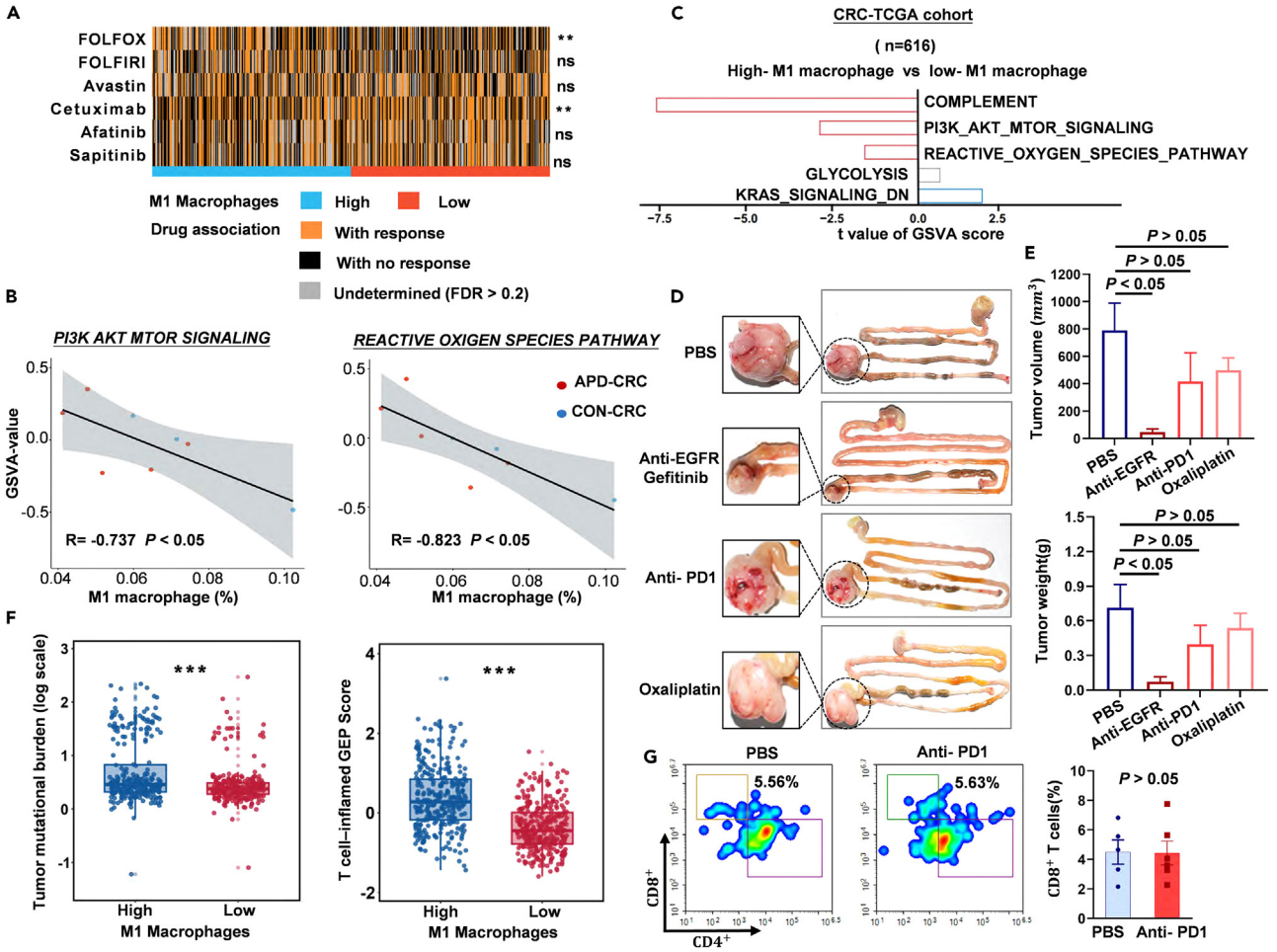

Figure 5. APD-CRC had a well response to cetuximab chemotherapy and poor response to anti-PD-1 immunotherapy

(A) Heatmap shows the association between individual CRC patient's responses to FOLFIRI, FOLFOX, EGFR inhibitors, and VEGF inhibitors in the TCGA CRC cohort. In these analyses, samples with an FDR <0.2 were regarded as significant. *$p < 0.05$, **$p < 0.01$, χ^2 test.

(B) PI3K AKT MTOR signaling and the reactive oxygen species pathway were significantly enriched in APD-CRC tissue with low-density M1 macrophages from mice.

(C) The pathway related to the density of M1 macrophage cells in CRC tissue from the TCGA cohort.

(D and E) Representative images of MC38 cecum orthotopic tumors from mice treated with PBS/gefitinib/anti-PD-1 antibody/oxaliplatin. Significant therapeutic effect was detected in mice who accepted gefitinib. There was no significant difference in tumor volumes and tumor weights in mice treated with PBS/anti-PD-1 antibody/oxaliplatin.

(F) TMB, defined as the sum of somatic nonsynonymous mutations, and T cell–inflamed GEP were assessed in the TCGA CRC cohort with a low or high density of M1 macrophage cells. *$p < 0.05$, **$p < 0.01$, ***$p < 0.001$, Wilcoxon test.

(G) Flow cytometric analysis of $CD8^+$ T cells in MC38 cecum orthotopic tumors from mice treated by PBS/anti-PD-1 antibody. Data are means ± SEM. The difference between the two groups was determined by a two-tailed Student's t test.

To verify that the poor prognosis of patients with APD-CRC may be related to the reduction of M1-type macrophages, we depleted the macrophage cells by clodronate liposomes treatment in mice bearing CT26 orthotopic tumor (Figure 4F). The depletion of macrophages was confirmed by flow cytometry on mouse spleen and tumor samples (Figures S4B and S4C). Consistently, similar levels of tumor size and tumor weight were detected in macrophage-depleted mice with or without appendectomy (Figures 4G, 4H, and S4D). These findings corroborated that the depletion of M1 macrophages caused by appendectomy contributes to a poor prognosis for CRC.

Patients with colorectal cancer with prior appendectomy had a well response to cetuximab chemotherapy and poor response to anti-PD-1 immunotherapy

The altered immune microenvironment of tumors induced by appendectomy may affect drug sensitivity. To find sensitive chemotherapy for patients with APD-CRC, we applied previous drug-gene signatures to gene expression profiles (GEPs) using the NTP algorithm,

including FOLFIRI, FOLFOX, and vascular endothelial growth factor (VEGF) or epidermal growth factor receptor (EGFR) inhibitors (Figure 5A). Specifically, the FOLFOX resistance signature was significantly (false discovery rate, FDR <0.2) associated with 63.4% (n = 161) of samples with the low density of M1 macrophage cells, as compared to only 49.8% (n = 123) of samples with a high density of M1 macrophage cells ($p < 0.01$) (Figure S5A). The lower score for FOLFOX signature sensitivity was also observed in CRC with low-density M1 macrophage cells compared with high density in Z score analysis (Figure S5B). Similar results that patients with CRC with low-density M1 macrophage cells had poor response to FOLFIRI could also be found both in NTP and Z score analysis (Figures 5A, S5A, and S5B, $p < 0.001$). Intriguingly, 59.2% of patients with CRC with low-density M1 macrophage cells responded to cetuximab, significantly more than cases with high-density M1 macrophage cells (48.5%, Figures 5A and S5A). There was no difference between the two groups in response to VEGF and HER2 inhibitors including Avastin, and Afatinib (Figures 5A and S5A). Moreover, the prediction of sensitive chemotherapy for patients with APD-CRC is supported by the analysis of enriched signaling pathways in APD-CRC. We analyzed RNA-sequencing data of CRC tissue from mice with or without appendectomy and TCGA CRC cohort (Figure S5C). The results identified that PI3K AKT MTOR signaling and reactive oxygen species pathway, reported to be associated with CRC development,[15,16] enriched in APD-CRC with low-density M1 macrophages. (Figure 5B). Consistently, the signaling pathways negatively related (*PI3K AKT MTOR signaling* and *reactive oxygen species pathway*) and positively related (*KRAS signaling down*) with the density of M1 macrophage cells were validated in TCGA CRC cohort by GSVA analysis (Figure 5C). This result supports the conclusion that patients with CRC with appendectomy are sensitive to cetuximab. The therapeutic efficacy of oxaliplatin and EGFR inhibitors was confirmed in appendectomy-mice bearing MC38 orthotopic tumors. The data suggested that gefitinib can effectively suppress the growth of tumors. While the tumor growth in mice treated with oxaliplatin was not significantly inhibited (Figures 5D, 5E, S5D, and S5E).

Tumor mutational burden (TMB) and T cell–inflamed GEP are emerging predictive biomarkers for immunotherapy. We also calculated the score of T cell–inflamed GEP and TMB to evaluate the effect of the density of M1 macrophage cells in CRC tissue on the sensitivity of immunotherapy. The results showed that CRC with low-density M1 macrophage cells has lower T cell–inflamed GEP scores and TMB, compared with the cases with a high density of M1 macrophage (Figure 5F). The result showed that patients with APD-CRC with the depletion of M1 macrophage cells were poorly responsive to immunotherapy. As expected, appendectomy-mice bearing MC38 orthotopic tumors were insensitive to anti-PD-1 therapy (Figures 5D and 5E). Both tumor weights and tumor sizes were not significantly different from those of control groups (Figures 5D, 5E, S5D, and S5E). Consistently, the proportion of infiltrating $CD8^+$ T cells in tumors from mice treated with anti-PD-1 antibody was similar to tumors from mice treated with PBS (Figure 5G). These results collectively revealed that patients with CRC with prior appendectomy had a well response to EGFR inhibitors chemotherapy and a poor response to anti-PD-1 immunotherapy.

DISCUSSION

Losing the normal function of the appendix, including chronic and acute appendicitis, appendectomy, and increased risk of CRC, has been suggested in different populations, such as the USA,[17] the United Kingdom,[18] France,[19] Swedish,[20] and Chinese.[7,9] However, appendicitis is the most common digestive surgical emergency in the world, which means that the oncologist might face a considerable number of patients with CRC with prior appendectomy. Our study focuses on the prognosis value and pathological characteristics of CRC that occurs after appendectomy, which is of great significance for the treatment of this population.

First, this study comprehensively evaluated the prognosis influence of prior appendectomy on patients with CRC based on a retrospective cohort study involving 4,214 subjects. It is worth mentioning that we excluded patients with CRC with IBD, because of their distinct tumors and patient-related factors.[21] More importantly, high-rate colon resection in IBD-CRC could increase the confounding bias.[22] The prior appendectomy was found to be significantly and independently associated with poor overall survival and disease-free survival of patients with CRC; especially right-sided colonic cancer, based on a multicentral CRC cohort.

Some studies have reported that prior appendectomy affected the stage of CRC,[23] but there was no study about the assessment of the prognostic significance of prior appendectomy for patients with CRC based on a large cohort. Our multicentral study observed that the prior appendectomy was significantly associated with poor OS and DFS, and the association was still unchanged after the adjustment of potential confounders (e.g., age, sex, smoking, alcohol, tumor location, tumor stage, tumor differentiation, family history of cancers, adjuvant radio/chemotherapy, R0 resection, comorbidity score). Considering the important role of the appendix in the gut's local protective immune response, there are several possible explanations for the positive association between prior appendectomy and the poor prognosis of proximal colon cancer. The weakened gut local immune response and immune surveillance after the removal of the appendix could be one of the possible reasons. These structures and lymphocytes indicate that the appendix is an important participant in gut antigen recognition and immune response to antigens (including CRC).[3] In addition, some evidence based on the murine model suggested there were a considerable amount of natural killer T lymphocytes in the appendix, which could elaborate on a series of chemokines and cytokines involved in gut immune response, including tumor-related immune response.[24] Therefore, the weakened gut local immunity caused by appendectomy could increase the risk of malignant changes in the large intestine, especially in the proximal colon, due to the adjacent anatomical sites and common embryological origins (midgut) shared with the appendix.

We further investigated the role of appendectomy in contributing to poor oncological outcomes in two CRC mouse models. Our results showed that appendectomy induces the depletion of M1 macrophages in CRC tissue from mice and patients. Kaplan-Meier survival analysis was conducted to evaluate the correlation between the density of M1 macrophages and OS outcomes in patients with colorectal adenocarcinoma using data from the TCGA database. It is noteworthy that the depletion of macrophages resulted in similar tumor sizes and weights in

mice, independent of appendectomy. Taken together, the depletion of M1 macrophages resulting from appendectomy may be the mechanism behind the poor prognosis for CRC induced by prior appendectomy.

As mentioned above, firstly, the decreased level of gut local immune response could partly explain the worse survival in patients with CRC with prior appendectomy. The important role of gut local immune responses in the prognosis of established CRC has been proposed for over 30 years. In the 1980s, Svennevig et al. proposed that local lymphoid infiltration could be a prognostic factor in colorectal carcinoma.[25] Subsequently, Halvorsen et al. found that the lack of local lymphocytic reaction was associated with unfavorable oncological outcomes.[26] Ogino et al., based on 843 patients with CRC from two independent cohorts, reported that an increasing lymphocytic reaction score (including Crohn's-like reaction, peritumoral reaction, intertumoral peri glandular reaction, and tumor-infiltrating lymphocytes) significantly correlated with favorable overall and CRC-specific survival.[27] Similar results were also reported by Rozek et al.[28] and Wallace et al.[29] Especially, TAMs with extremely high plasticity are the most abundant immune cells in the TME. Classical M1 polarization has been defined by the expression of CD80, CD86, MHCII, iNOS, and CD68, correlated with the tumoricidal function of TAMs that could engulf cancer cells and recruit T cells.[30] M1 macrophages enriched in tumors are positively linked to better survival outcomes, which has also been observed in lung cancers.[31]

CRC is highly heterogeneous, and paying attention to the TME has made great contributions to improving drug resistance, cancer metastasis, and treatment failure.[32] Given the important role of M1 macrophage cells in appendectomy-CRC tumorigenesis and prognosis, we explored effective treatment for CRC with prior appendectomy. This will provide a reference for developing treatment plans for the considerable number of patients with appendectomy-associated colorectal cancer (APD-CRC), which is of great clinical significance. Our results demonstrated that patients with CRC with lower M1 macrophage cells have a response to EGFR inhibitors, such as cetuximab. Furthermore, we further identified some important pro-carcinogenic signaling pathways, including *PI3K AKT MTOR* signaling and reactive oxygen species pathways, that are negatively related to the density of M1 macrophage cells. This provides support for the results showing that APD-CRC will respond to EGFR inhibitors.

Furthermore, our study found that APD-CRC with a low density of M1 macrophage cells displays lower T cell-inflamed GEP scores and TMB, which meant that these patients had features insensitive to immunotherapy. Immune checkpoint blockade (ICB) therapy has become the main immunotherapy for CRC. The tumor immune microenvironment is the main determinant of ICB response,[33] including TAMs.[34] Activated T cells in the tumor immune microenvironment skew macrophages into late-stage activated M1-like macrophages, and late-stage activated M1-like macrophages are critical for effective tumor control.[35] Weissleder R etc. developed TLR7/8-agonist-loaded nanoparticles with efficient modulating the polarization of TAMs toward the M1 phenotype to enhance cancer immunotherapy.[36] The study suggested that the disruption of M2 macrophage trafficking sensitizes hepatocellular carcinoma to anti-PD-L1 blockade.[37]

In conclusion, losing the normal function of the appendix could be an independent risk factor for the prognosis of patients with CRC. Mechanistically, appendectomy causes the depletion of M1 macrophages in tumor tissue, which contributes to the appendectomy-induced poor prognosis for CRC. APD-CRC with a lower density of M1 macrophages responds well to EGFR inhibitors and poorly to immunotherapy. This study provides insights into the function of the appendix by regulating the infiltration of TAMs in CRC tissue, thus suggesting clinicians choose appropriate drugs to improve the prognosis of patients with APD-CRC based on the change in TME.

Limitations of the study

This study has several limitations. First, this is a retrospective cohort and potential unknown confounding factors may introduce selection bias that was not adjusted or matched. Nevertheless, our results remained robust in both the adjusted Cox regression model and propensity score-matched cohort. Some variables lack more detailed information, such as the regimen and dosage of radiotherapy and chemotherapy, and so forth. Second, the multicentral CRC cohort used in the study might not represent a diverse population, limiting the generalizability of the findings. Besides, the exploration of the mechanism and prediction of sensitive therapy was mostly based on mouse models, which is not enough to guide clinical medication. There is no doubt that more retrospective and prospective studies with larger sample sizes, different ethnicities, more detailed information on potential confounders, and long-term follow-up are warranted to confirm our findings.

STAR★METHODS

Detailed methods are provided in the online version of this paper and include the following:

- KEY RESOURCES TABLE
- RESOURCE AVAILABILITY
  - Lead contact
  - Materials availability
  - Data and code availability
- EXPERIMENTAL MODEL AND STUDY PARTICIPANT DETAILS
  - Ethics approval and consent to participate
  - Cell lines
  - Animals
  - Patients and clinical specimens

SUPPLEMENTAL INFORMATION

Supplemental information can be found online at https://doi.org/10.1016/j.isci.2024.110578.

ACKNOWLEDGMENTS

We acknowledge the work of the biobank in The First Affiliated Hospital of Xi'an Jiao Tong University and Xijing Hospital. This project was supported by the National Natural Science Foundation of China (No. 81870380 and No. 82303941), Shaanxi Province Science Foundation (2020ZDLSF01-03), and Integrative "Basic-Clinical" Innovation Program (YXJLRH2022043).

AUTHOR CONTRIBUTIONS

The work reported in the article has been performed by the authors unless clearly specified in the text.

G.J. and J.S. conceived the study. G.L. and F.S. planned and designed experiments. G.L., C.H., Q.L., R.W., and F.S. performed experiments. G.L., J.W., Q.L., J.Z., Z.Z., P.Q., Z.C., and F.S. collected data. G.L. and F.S. wrote and edited the article. J.S. and F.S. supplied resources. All authors have read, edited, and approved the final article.

DECLARATION OF INTERESTS

The authors declare no competing interests.

Received: March 9, 2024
Revised: June 15, 2024
Accepted: July 22, 2024
Published: July 25, 2024

REFERENCES

1. Dekker, E., Tanis, P.J., Vleugels, J.L.A., Kasi, P.M., and Wallace, M.B. (2019). Colorectal cancer. Lancet *394*, 1467–1480. https://doi.org/10.1016/S0140-6736(19)32319-0.
2. Torpy, J.M., Burke, A.E., and Golub, R.M. (2011). Appendectomy. JAMA *306*, 2404. https://doi.org/10.1001/jama.2011.767.
3. Girard-Madoux, M.J.H., Gomez de Agüero, M., Ganal-Vonarburg, S.C., Mooser, C., Belz, G.T., Macpherson, A.J., and Vivier, E. (2018). The immunological functions of the Appendix: An example of redundancy? Semin. Immunol. *36*, 31–44. https://doi.org/10.1016/j.smim.2018.02.005.
4. Kooij, I.A., Sahami, S., Meijer, S.L., Buskens, C.J., and te Velde, A.A. (2016). The immunology of the vermiform appendix: a review of the literature. Clin. Exp. Immunol. *186*, 1–9. https://doi.org/10.1111/cei.12821.
5. Vitetta, L., Chen, J., and Clarke, S. (2019). The vermiform appendix: an immunological organ sustaining a microbiome inoculum. Clin. Sci. *133*, 1–8. https://doi.org/10.1042/CS20180956.
6. Lai, H.W., Loong, C.C., Tai, L.C., Wu, C.W., and Lui, W.Y. (2006). Incidence and odds ratio of appendicitis as first manifestation of colon cancer: a retrospective analysis of 1873 patients. J. Gastroenterol. Hepatol. *21*, 1693–1696. https://doi.org/10.1111/j.1440-1746.2006.04426.x.
7. Wu, S.C., Chen, W.T.L., Muo, C.H., and Sung, F.C. (2015). Appendicitis as an Early Manifestation of Subsequent Malignancy: An Asian Population Study. PLoS One *10*, e0122725. https://doi.org/10.1371/journal.pone.0122725.
8. Wu, S.C., Chen, W.T.L., Muo, C.H., Ke, T.W., Fang, C.W., and Sung, F.C. (2015). Association between appendectomy and subsequent colorectal cancer development: an Asian population study. PLoS One *10*, e0118411. https://doi.org/10.1371/journal.pone.0118411.
9. Shi, F., Liu, G., Lin, Y., Guo, C.L., Han, J., Chu, E.S.H., Shi, C., Li, Y., Zhang, H., Hu, C., et al. (2023). Altered gut microbiome composition by appendectomy contributes to colorectal cancer. Oncogene *42*, 530–540. https://doi.org/10.1038/s41388-022-02569-3.
10. Fan, Z., Liu, Y., Li, C., Jiang, Y., Wang, N., Wang, M., Li, C., Diao, Y., Qiu, W., Zhu, X., et al. (2024). T proliferating cells derived

autophagy signature associated with prognosis and immunotherapy resistance in a pan-cancer analysis. iScience *27*, 108701. https://doi.org/10.1016/j.isci.2023.108701.
11. Christofides, A., Strauss, L., Yeo, A., Cao, C., Charest, A., and Boussiotis, V.A. (2022). The complex role of tumor-infiltrating macrophages. Nat. Immunol. *23*, 1148–1156. https://doi.org/10.1038/s41590-022-01267-2.
12. Morad, G., Helmink, B.A., Sharma, P., and Wargo, J.A. (2022). Hallmarks of response, resistance, and toxicity to immune checkpoint blockade. Cell *185*, 576. https://doi.org/10.1016/j.cell.2022.01.008.
13. Neufert, C., Becker, C., and Neurath, M.F. (2007). An inducible mouse model of colon carcinogenesis for the analysis of sporadic and inflammation-driven tumor progression. Nat. Protoc. *2*, 1998–2004. https://doi.org/10.1038/nprot.2007.279.
14. Liu, X., Mao, B., Gu, J., Wu, J., Cui, S., Wang, G., Zhao, J., Zhang, H., and Chen, W. (2021). *Blautia*-a new functional genus with potential probiotic properties? Gut Microb. *13*, 1–21. https://doi.org/10.1080/19490976.2021.1875796.
15. LoRusso, P.M. (2016). Inhibition of the PI3K/AKT/mTOR Pathway in Solid Tumors. J. Clin. Oncol. *34*, 3803–3815. https://doi.org/10.1200/JCO.2014.59.0018.
16. Peng, L., Jiang, J., Chen, H.N., Zhou, L., Huang, Z., Qin, S., Jin, P., Luo, M., Li, B., Shi, J., et al. (2021). Redox-sensitive cyclophilin A elicits chemoresistance through realigning cellular oxidative status in colorectal cancer. Cell Rep. *37*, 110069. https://doi.org/10.1016/j.celrep.2021.110069.
17. Dahabra, L., Tallat, M., Abouyassine, A., and Deeb, L. (2021). S134 Does Appendectomy Alter the Risk of Colorectal Cancer? A Large Population-Based Study in the United States. Am. J. Gastroenterol. *116*, S58–S59. https://doi.org/10.14309/01.ajg.0000773008.85391.1b.
18. Hajibandeh, S., Hajibandeh, S., Morgan, R., and Maw, A. (2020). The incidence of right-sided colon cancer in patients aged over 40 years with acute appendicitis: A systematic review and meta-analysis. Int. J. Surg. *79*, 1–5. https://doi.org/10.1016/j.ijsu.2020.04.065.
19. Viennet, M., Tapia, S., Cottenet, J., Bernard, A., Ortega-Deballon, P., and Quantin, C. (2023). Increased risk of colon cancer after acute appendicitis: a nationwide, population-based study. EClinicalMedicine *63*, 102196. https://doi.org/10.1016/j.eclinm.2023.102196.
20. Song, H., Abnet, C.C., Andrén-Sandberg, Å., Chaturvedi, A.K., and Ye, W. (2016). Risk of Gastrointestinal Cancers among Patients with Appendectomy: A Large-Scale Swedish Register-Based Cohort Study during 1970-2009. PLoS One *11*, e0151262. https://doi.org/10.1371/journal.pone.0151262.
21. Ording, A.G., Horváth-Puhó, E., Erichsen, R., Long, M.D., Baron, J.A., Lash, T.L., and Sørensen, H.T. (2013). Five-year mortality in colorectal cancer patients with ulcerative colitis or Crohn's disease: a nationwide population-based cohort study. Inflamm. Bowel Dis. *19*, 800–805. https://doi.org/10.1097/MIB.0b013e3182802af7.
22. Birch, R.J., Burr, N., Subramanian, V., Tiernan, J.P., Hull, M.A., Finan, P., Rose, A., Rutter, M., Valori, R., Downing, A., and Morris, E.J.A. (2022). Inflammatory Bowel Disease-Associated Colorectal Cancer Epidemiology and Outcomes: An English Population-Based Study. Am. J. Gastroenterol. *117*, 1858–1870. https://doi.org/10.14309/ajg.0000000000001941.
23. Ábrahám, S., Németh, T., Benkő, R., Matuz, M., Ottlakán, A., Váczi, D., Paszt, A., Simonka, Z., and Lázár, G. (2020). Evaluating the distribution of the locations of colorectal cancer after appendectomy and cholecystectomy. World J. Surg. Oncol. *18*, 94. https://doi.org/10.1186/s12957-020-01861-4.
24. Ishimoto, Y., Tomiyama-Miyaji, C., Watanabe, H., Yokoyama, H., Ebe, K., Tsubata, S., Aoyagi, Y., and Abo, T. (2004). Age-dependent variation in the proportion and number of intestinal lymphocyte subsets, especially natural killer T cells, double-positive CD4+ CD8+ cells and B220+ T cells, in mice. Immunology *113*, 371–377. https://doi.org/10.1111/j.1365-2567.2004.01961.x.
25. Svennevig, J.L., Lunde, O.C., and Holter, J. (1982). In Situ Analysis of the Inflammatory Cell Infiltrates in Colon Carcinomas and in the Normal Colon Wall. Acta Pathol. Microbiol. Immunol. Scand. A *90*, 131–137. https://doi.org/10.1111/j.1699-0463.1982.tb00073_90A.x.
26. Halvorsen, T.B., and Seim, E. (1989). Association between invasiveness, inflammatory reaction, desmoplasia and survival in colorectal cancer. J. Clin. Pathol. *42*, 162–166. https://doi.org/10.1136/jcp.42.2.162.
27. Ogino, S., Nosho, K., Irahara, N., Meyerhardt, J.A., Baba, Y., Shima, K., Glickman, J.N., Ferrone, C.R., Mino-Kenudson, M., Tanaka, N., et al. (2009). Lymphocytic Reaction to Colorectal Cancer Is Associated with Longer Survival, Independent of Lymph Node Count, Microsatellite Instability, and CpG Island Methylator Phenotype. Clin. Cancer Res. *15*, 6412–6420. https://doi.org/10.1158/1078-0432.Ccr-09-1438.
28. Rozek, L.S., Schmit, S.L., Greenson, J.K., Tomsho, L.P., Rennert, H.S., Rennert, G., and Gruber, S.B. (2016). Tumor-Infiltrating Lymphocytes, Crohn's-Like Lymphoid Reaction, and Survival From Colorectal Cancer. J. Natl. Cancer Inst. *108*, djw027. https://doi.org/10.1093/jnci/djw027.
29. Wallace, K., Lewin, D.N., Sun, S., Spiceland, C.M., Rockey, D.C., Alekseyenko, A.V., Wu, J.D., Baron, J.A., Alberg, A.J., and Hill, E.G. (2018). Tumor-Infiltrating Lymphocytes and Colorectal Cancer Survival in African American and Caucasian Patients. Cancer Epidemiol. Biomarkers Prev. *27*, 755–761. https://doi.org/10.1158/1055-9965.Epi-17-0870.
30. Martinez, F.O., Sica, A., Mantovani, A., and Locati, M. (2008). Macrophage activation and polarization. Front. Biosci. *13*, 453–461. https://doi.org/10.2741/2692.
31. Garrido-Martin, E.M., Mellows, T.W.P., Clarke, J., Ganesan, A.-P., Wood, O., Cazaly, A., Seumois, G., Chee, S.J., Alzetani, A., King, E.V., et al. (2020). M1^{hot} tumor-associated macrophages boost tissue-resident memory T cells infiltration and survival in human lung cancer. J. Immunother. Cancer *8*, e000778. https://doi.org/10.1136/jitc-2020-000778.
32. Chao, S., Zhang, F., Yan, H., Wang, L., Zhang, L., Wang, Z., Xue, R., Wang, L., Wu, Z., Jiang, B., et al. (2023). Targeting intratumor heterogeneity suppresses colorectal cancer chemoresistance and metastasis. EMBO Rep. *24*, e56416. https://doi.org/10.15252/embr.202256416.
33. Ganesh, K., Stadler, Z.K., Cercek, A., Mendelsohn, R.B., Shia, J., Segal, N.H., and Diaz, L.A., Jr. (2019). Immunotherapy in colorectal cancer: rationale, challenges and potential. Nat. Rev. Gastroenterol. Hepatol. *16*, 361–375. https://doi.org/10.1038/s41575-019-0126-x.
34. Meyiah, A., Alahdal, M., and Elkord, E. (2023). Role of exosomal ncRNAs released by M2 macrophages in tumor progression of gastrointestinal cancers. iScience *26*, 106333. https://doi.org/10.1016/j.isci.2023.106333.
35. van Elsas, M.J., Middelburg, J., Labrie, C., Roelands, J., Schaap, G., Sluijter, M., Tonea, R., Ovcinnikovs, V., Lloyd, K., Schuurman, J., et al. (2024). Immunotherapy-activated T cells recruit and skew late-stage activated M1-like macrophages that are critical for therapeutic efficacy. Cancer Cell *42*, 1032–1050.e10. https://doi.org/10.1016/j.ccell.2024.04.011.
36. Rodell, C.B., Arlauckas, S.P., Cuccarese, M.F., Garris, C.S., Li, R., Ahmed, M.S., Kohler, R.H., Pittet, M.J., and Weissleder, R. (2018). TLR7/8-agonist-loaded nanoparticles promote the polarization of tumour-associated macrophages to enhance cancer immunotherapy. Nat. Biomed. Eng. *2*, 578–588. https://doi.org/10.1038/s41551-018-0236-8.
37. Zhu, Y., Yang, J., Xu, D., Gao, X.M., Zhang, Z., Hsu, J.L., Li, C.W., Lim, S.O., Sheng, Y.Y., Zhang, Y., et al. (2019). Disruption of tumour-associated macrophage trafficking by the osteopontin-induced colony-stimulating factor-1 signalling sensitises hepatocellular carcinoma to anti-PD-L1 blockade. Gut *68*, 1653–1666. https://doi.org/10.1136/gutjnl-2019-318419.
38. Ho, D.E., Imai, K., King, G., and Stuart, E.A. (2017). Matching as Nonparametric Preprocessing for Reducing Model Dependence in Parametric Causal Inference. Polit. Anal. *15*, 199–236. https://doi.org/10.1093/pan/mpl013.
39. Ho, D.E., Imai, K., King, G., and Stuart, E.A. (2011). MatchIt: Nonparametric Preprocessing for Parametric Causal Inference. J. Stat. Softw. *42*, 1–28. https://doi.org/10.18637/jss.v042.i08.
40. Austin, P.C. (2009). Balance diagnostics for comparing the distribution of baseline covariates between treatment groups in propensity-score matched samples. Stat. Med. *28*, 3083–3107. https://doi.org/10.1002/sim.3697.
41. Li, Y., Liu, J., Liu, G., Pan, Z., Zhang, M., Ma, Y., Wei, Q., Xia, H., Zhang, R.X., and She, J. (2019). Murine Appendectomy Model of Chronic Colitis Associated Colorectal Cancer by Precise Localization of Caecal Patch. J. Vis. Exp. *150*, e59921. https://doi.org/10.3791/59921.
42. Patro, R., Duggal, G., Love, M.I., Irizarry, R.A., and Kingsford, C. (2017). Salmon provides fast and bias-aware quantification of transcript expression. Nat. Methods *14*, 417–419. https://doi.org/10.1038/nmeth.4197.
43. Kasashima, H., Duran, A., Cid-Diaz, T., Muta, Y., Kinoshita, H., Batlle, E., Diaz-Meco, M.T., and Moscat, J. (2021). Mouse model of colorectal cancer: orthotopic co-implantation of tumor and stroma cells in cecum and rectum. STAR Protoc. *2*, 100297. https://doi.org/10.1016/j.xpro.2021.100297.

44. Zhang, Z., Chen, C., Yang, F., Zeng, Y.X., Sun, P., Liu, P., and Li, X. (2022). Itaconate is a lysosomal inducer that promotes antibacterial innate immunity. Mol. Cell *82*, 2844–2857.e10. https://doi.org/10.1016/j.molcel.2022.05.009.

45. Wong, S.H., Kwong, T.N.Y., Chow, T.C., Luk, A.K.C., Dai, R.Z.W., Nakatsu, G., Lam, T.Y.T., Zhang, L., Wu, J.C.Y., Chan, F.K.L., et al. (2017). Quantitation of faecal *Fusobacterium* improves faecal immunochemical test in detecting advanced colorectal neoplasia. Gut *66*, 1441–1448. https://doi.org/10.1136/gutjnl-2016-312766.

46. Hoshida, Y. (2010). Nearest template prediction: a single-sample-based flexible class prediction with confidence assessment. PLoS One *5*, e15543. https://doi.org/10.1371/journal.pone.0015543.

47. Zhu, X., Tian, X., Ji, L., Zhang, X., Cao, Y., Shen, C., Hu, Y., Wong, J.W.H., Fang, J.Y., Hong, J., and Chen, H. (2021). A tumor microenvironment-specific gene expression signature predicts chemotherapy resistance in colorectal cancer patients. NPJ Precis. Oncol. *5*, 7. https://doi.org/10.1038/s41698-021-00142-x.

48. Cristescu, R., Mogg, R., Ayers, M., Albright, A., Murphy, E., Yearley, J., Sher, X., Liu, X.Q., Lu, H., Nebozhyn, M., et al. (2018). Pan-tumor genomic biomarkers for PD-1 checkpoint blockade-based immunotherapy. Science *362*, eaar3593. https://doi.org/10.1126/science.aar3593.

49. Mayakonda, A., Lin, D.C., Assenov, Y., Plass, C., and Koeffler, H.P. (2018). Maftools: efficient and comprehensive analysis of somatic variants in cancer. Genome Res. *28*, 1747–1756. https://doi.org/10.1101/gr.239244.118.

STAR★METHODS

KEY RESOURCES TABLE

REAGENT or RESOURCE	SOURCE	IDENTIFIER
Antibodies		
PE anti-mouse CD86	BioLegend	Cat# 105007; RRID: AB_313150
PerCP-Cy5.5 anti-mouseCD11b	BioLegend	Cat# 101227; RRID: AB_893233
AF488 anti-mouse F4/80	BioLegend	Cat# 123119; RRID: AB_893491
Brilliant Violet 605™ anti-mouse CD45 Antibody	BioLegend	Cat#157217; RRID: AB_3097472
PE anti-mouse CD3 Antibody	BioLegend	Cat#100205; RRID: AB_312662
Brilliant Violet 421™ anti-mouse CD8 Antibody	BioLegend	Cat#100737: RRID: AB_10897101
PerCP/Cyanine5.5 anti-mouse CD4 Antibody	BioLegend	Cat#100433; RRID: AB_893330
CD80	Proteintech	Cat#66406-1-Ig; RRID: AB_2827408
iNOS	Abcam	Cat#ab283655; RRID: AB_3083470
Biological samples		
Human CRC samples	the First Affiliated Hospital of Xi'an Jiaotong University	NA
Chemicals, peptides, and recombinant proteins		
clodronate liposome	Yeasen	Cat#40337ES10
collagenase IV	Solarbio	Cat# C8160
Bovine Serum Albumin	Solarbio	Cat#A8010
DNase	Roche	CAS#9003-98-9
dextran sulfate sodium	MP Biomedicals	CAS#0216011080
azoxymethane	MCE	CAS#HY-111375
Oxaliplatin	MCE	Cat #HY-17371
Gefitinib	MCE	Cat #HY-50895
Anti-Mouse PD-1 antibody	MCE	Cat #HY-P99144
Critical commercial assays		
QIAamp DNA Mini kit	Qiagen	CAT#56304
Deposited data		
CRC from mouse RNA-seq data	This study	BioProject: PRJNA1008680
CRC from mouse RNA-seq data	This study	BioProject: PRJNA906334
CRC from human RNA-seq data	This study	GSA-Human: HRA005817
CRC from human RNA-seq data	This study	GSA-Human: HRA006295
Experimental models: Cell lines		
MC38	Cell Resource Center, Peking Union Medical College (PCRC)	1101MOU-PUMC000523
CT26	National Collection of Authenticated Cell Cultures	TCM37
Experimental models: Organisms/strains		
C57BL/6 mice	Beijing Vital River Laboratory Animal Technology Co., Ltd.	NA
BALB/c mice	Beijing Vital River Laboratory Animal Technology Co., Ltd.	NA

(*Continued on next page*)

Continued

REAGENT or RESOURCE	SOURCE	IDENTIFIER
Software and algorithms		
NovoExpress 1.6.0	Agilent Technologies	https://www.agilent.com.cn/zh-cn/product/research-flow-cytometry/flow-cytometry-software/novocyte-novoexpress-software-1320805
GraphPad Prism 9.3.0 software	GraphPad	https://www.graphpad.com
R V.4.0.2	R Core Team	https://www.r-project.org/
IBM SPSS statistic 26	IBM	https://www.ibm.com/cn-zh/spss

RESOURCE AVAILABILITY

Lead contact

Further information and requests for resources and reagents should be directed to and will be fulfilled by the Lead Contact, Feiyu Shi, (011357@xjtufh.edu.cn).

Materials availability

This study did not generate new materials.

Data and code availability

- Data: The raw sequence data of tumors from mice are available in the Sequence Read Archive (SRA) of the U.S. National Center for Biotechnology Information (BioProject: PRJNA906334, PRJNA1008680). And the raw sequence data of tumor from CRC patients reported in this paper have been deposited in the Genome Sequence Archive (Genomics, Proteomics & Bioinformatics 2021) in National Genomics Data Center (Nucleic Acids Res 2022), China National Center for Bioinformation / Beijing Institute of Genomics, Chinese Academy of Sciences (GSA-Human: HRA005817, HRA006295) that are publicly accessible at https://ngdc.cncb.ac.cn/gsa.
- Code: This paper does not report original code.
- All other requests: Any additional information required to reanalyze the data reported in this work paper is available from the lead contact upon request.

EXPERIMENTAL MODEL AND STUDY PARTICIPANT DETAILS

Ethics approval and consent to participate

This study was approved by the institutional review board of The First Affiliated Hospital of Xi'an Jiao Tong University and Xijing hospital (Xi'An, China; approval number, XJTUIAF2019LSK-227[June 1, 2019]). All animal procedures were approved by the Institutional Animal Care and Use Committee of Xi'an Jiaotong University (Xi'an, China; approval number, XJTULAC2019-1023).

Cell lines

MC38 cells, obtained from Cell Resource Center Peking Union Medical College (PCRC), were maintained in Dulbecco's modified Eagle's medium (DMEM) supplemented with 10% fetal bovine serum (FBS). And CT26 cells obtained from National Collection of Authenticated Cell Cultures were cultured in RPMI-1640 medium supplemented with 10% FBS. All cells were maintained in a humidified incubator equilibrated with 5% CO2 at 37°C unless otherwise stated.

Animals

Five-week-old male C57BL/6J mice and five-week-old male BALB/c mice were purchased from Beijing Vital River Laboratory Animal Technology Co., Ltd. In each group, 5/6 mice were utilized to observe the tumor phenotype changes and analyzed for M1 macrophages by flow cytometry. And there are 5 mice in each group for treatment. Animal handling and procedures were approved by Institutional Animal Care and Use Committee of Xi'an Jiaotong University (Xi'an, China; approval number, XJTULAC2019-1023).

Patients and clinical specimens

Fresh tumor tissues were obtained from surgical specimens from patients with colorectal cancer in the First Affiliated Hospital of Xi'an Jiaotong University (n=123, 57.7% male, age: 63.4±10.5 years). Samples were frozen in liquid nitrogen immediately after surgical removal and maintained at -80°C. Paraffin-embedded sections of colorectal tumor were obtained from the Pathology Department of the First Affiliated Hospital of Xi'an Jiaotong University (n=74, 60.8% male, age: 65.7±11.6 years). There were no restrictions on race or ethnicity and all patients who were included were Chinese. This study was approved by the Ethics Committee of Xi'an Jiao Tong University, and conducted in accordance with the Helsinki Declaration.

METHOD DETAILS

Study design and patient selection

We conducted a multi-center retrospective cohort study. We enrolled all consecutive CRC patients with histologically confirmed adenocarcinoma from January 2013 to January 2019 at The First Affiliated Hospital of Xi'an Jiaotong University (Xi'an, Shaanxi) and from May 2010 to September 2016 at Xijing Hospital (Xi'an, Shaanxi). Our exclusion criteria included: 1. CRC Patients with age ≤18 years old; 2. CRC Patients with hereditary syndromes (e.g. Lynch syndrome and familial adenomatous polyposis); 3. Patients with any history of malignant disease, and inflammatory bowel disease (IBD) before the diagnosis of colorectal cancer; 4. Patients with multiple primary colorectal carcinoma or recurrent CRC, and other kinds of cancers; 5. Patients with any appendiceal neoplasms; 6. Patients with the diagnosis of colorectal cancer within 12 months of post-appendectomy; 7. Patients underwent appendectomy after the diagnosis of colorectal cancer. Finally, 4,214 CRC patients were included in this study for further analysis. The flow charts of patients screening and grouping in the cohort are depicted in Figure S1.

Study covariates

The clinical data of all included patients were obtained from Biobank of the First Affiliated Hospital of Xi'an Jiao Tong University and Xi Jing Hospital, including basic characteristics (age at diagnosis, gender, past medical history, smoking status, alcohol status, family cancer history, comorbidity (based on Charlson comorbidity index score (CCI)), treatment (chemo/radiotherapy, surgery or other), and Clinicopathological parameters (primary tumor location, pathological diagnosis, histological grade, TNM stage). The follow-up data (adjuvant therapy, survival status, tumor progression status, and death) were available until March 1, 2020 (First Affiliated Hospital of Xi'an Jiao Tong University) or April 1, 2017 (Xi Jing Hospital). The prior appendectomy was defined as patients who underwent appendectomy before CRC diagnosis at least 12 months, which was accessed by operation history in inpatient medical records and abdominal CT images during hospitalization for CRC.

Study objectives and outcomes

The study aimed to explore the possible association between prior appendectomy and survival (OS and DFS) of colorectal cancer patients. We divided CRC into 3 groups according to the cancer location: right-sided colon cancer, left-sided colon cancer, rectal cancer. Right-sided colon cancer includes cancer at the cecum, ascending colon, hepatic flexure, and transverse colon. Left-sided colon cancer includes cancer at the splenic flexure, descending colon, and sigmoid colon. DFS was followed from the CRC diagnosis until relapse (local and distant recurrence or metastasis with imaging or histological evidence), death or March 1, 2020 (First Affiliated Hospital of Xi'an Jiao Tong University) or April 1, 2017 (Xi Jing Hospital), whichever came first. These subjects with palliative resection and stage IV tumors were not included in DFS.

Details of propensity score matching

Propensity score matching was performed using R V.4.0.2 (R Foundation for Statistical Computing) statistical software and MatchIt package V.4.1.0.[38,39] We established a logistic regression model to calculate the propensity score conditional on the age and sex to represent the probability of appendectomy. Appendectomy patients were matched to non-appendectomy individuals in a 1:5 ratio without replacement using a greedy distance-based matching algorithm within a caliper width of 0.02. We assessed the balance of the covariates between the two groups by using absolute standardized difference (ASD). The ASD was calculated by the formula in the previous literature.[40]

For continuous variables, the ASD is defined as

$$ASD = \frac{\overline{x}_{treatment} - \overline{x}_{control}}{\sqrt{\frac{s^2_{treatment} + s^2_{control}}{2}}}$$

where $\overline{x}_{treatment}$ and $\overline{x}_{control}$ denote the sample mean of the covariate in treated and untreated subjects, respectively, while $s^2_{treatment}$ and $s^2_{control}$ denote the sample variance of the covariate in treated and untreated subjects, respectively.

For dichotomous variables, the ASD is defined as

$$ASD = \frac{p_{treatment} - p_{control}}{\sqrt{\frac{p_{treatment}(1 - p_{treatment}) + p_{control}(1 - p_{control})}{2}}}$$

where $p_{treatment}$ and $p_{control}$ denote the prevalence or mean of the dichotomous variable in treated and untreated subjects, respectively.

An ASD of < 0.20 indicates good balance for that particular variable.

Statistical analysis for cohort study

All statistical analyses were performed using R statistical software (version 4.0.2). Continuous variables were expressed as mean ± standard deviation (SD) or median (inter-quartile range (IQR)) according to the normality of data. The Cox proportional hazard regression model was applied to examine whether the prior appendectomy could serve as a risk factor for OS or DFS in CRC patients. Multivariable-adjusted HR was calculated. The confounders adjusted in the regression models include age, sex, smoking status, alcohol status, CRC family history of cancers, tumor stage, tumor differentiation, Adjuvant radio/chemotherapy, and CCI score. All statistical tests were two-sided and a p value less than 0.05 was considered statistically significant.

We also conducted sensitivity analyses to evaluate the robustness of the results. Firstly, we established a sensitivity analysis dataset for unmatched data and analyzed the main results. Then, we performed the sensitivity analysis and calculated the main results based on the data from the First Affiliated Hospital of Xi'an Jiaotong University.

Azoxymethane/dextran sulfate sodium-induced CRC mice model

Male C57BL/6 mice (5 weeks old) were housed in a certified specific-pathogen-free (SPF) environment. The mice were randomly divided into two groups: the appendectomy group, which received surgical removal of the appendix lymphoid, and the control group, which underwent an abdominal incision as control. The induction of colorectal cancer in mice in both groups was performed 7 days after surgery, following the procedure described in our previous study.[41] In brief, the mice were fed a diet supplemented with 2% dextran sulfate sodium (DSS) for one week, followed by a normal diet for 2 weeks. This induction cycle was repeated 6 times. It is noteworthy that a single intraperitoneal injection of azoxymethane (AOM) at a dose of 0.01 mg/g was administered only on the first day before the first induction cycle. At the end of the induction period, the remaining mice from the two groups were euthanized. Colonic tumors and adjacent normal tissue were then sampled and stored in 10% buffered formalin or liquid nitrogen for subsequent analysis.

RNA sequencing and analysis

Total RNA was extracted from mouse colon tumor tissues. The generation and sequencing of cDNA libraries were performed on the NovaSeq 6000 platform to generate 150bp paired-end reads. Clean RNA-seq reads were mapped to the Mouse transcriptome (mM10, GRCm38) and quantified at the gene level using Salmon[42] with GENCODE (vM22) gene annotations. We considered differentially expressed genes (DEG) between two groups of samples when the DESeq2 analysis resulted in an adjusted pp-value ≤ 0.05 and the fold-change (FC) in gene expression was ≥ 2. Analysis of molecular pathways affected by DEGs was performed using the KEGG/GO Analysis tool. CIBERSORT (https://cibersortx.stanford.edu/) was utilized to compute immune cell infiltration in samples. This was performed to quantify the relative proportions of infiltrating immune cells based on the gene expression profiles observed in samples. A reference set consisting of 22 distinct immune cell subtypes (LM22) and 1000 different permutations was utilized to estimate the potential number of immune cells. The sequencing coverage and quality statistics for each sample are summarized in Table S12.

Immunohistochemistry staining

The density of M1 macrophages in tumor tissue was assessed using immunohistochemistry (IHC) for CD80 and iNOS. Staining for CD80 (Proteintech, #66406-1-Ig) / iNOS (Abcam, #ab283655) was performed on paraffin-embedded sections of mice colon tumor from both appendectomy and control mice, as well as tumor specimens surgically resected from CRC patients with or without a history of appendectomy. A total of 74 tumor samples from CRC patients (37 appendectomy-CRC cases and 37 age-, gender-, and location-matched control-CRC cases) were collected. All subjects signed the informed consent forms before the sample collection.

Images were captured using Case Viewer. The density of M1 macrophages was determined by counting the proportion of cells that stained expression for CD80 and iNOS in tumor tissue using ImageJ software. Five random microscopic fields were analyzed for each sample.

Cell culture

Mouse CRC cell lines CT26 (RRID: CVCL_7254) were stably transfected with the firefly luciferase gene by lentivirus. CT26-Luci cells were cultured in RPMI-1640 and MC38 (RRID: CVCL_B288) were cultured in DMEM with 10% fetal bovine serum (FBS), maintained under saturated humidity, 37°C, 5% CO2 conditions, digested and passaged with 0.25% trypsin, and logarithmic growth phase cells were taken for animal experiments.

Orthotopic mouse models of colorectal cancer

A 10ul CT26-Luci cells suspension of equivalent to $5*10^5$ cells was orthotopically injected into the colonic serosa of male BALB/c mice (aged 5 weeks) with or without appendectomy respectively.[43] The fluorescence intensity of tumor cells in BALB/c mice was observed using a small animal live imaging system (IVIS®Lumina III) on the 7^{th}, 14^{th}, 21^{st} after cell injection. Two groups of mice were euthanized and the whole intestine tract was harvested 30 days after injection.

A 10ul MC38 cells suspension of equivalent to 1*106 cells was orthotopically injected into the colonic serosa of male C57BL/6 (aged 5 weeks) with appendectomy. Then, these mice were randomly divided into 4 groups for drug treatment 10 days after accepting the injection of cells.

Oxaliplatin (2mg/kg, MCE, #HY-17371) were intraperitoneally injected once every three days. It is worth noting that after administering 5mg/kg oxaliplatin twice, the mice suffered intolerance, and the dose was changed 2mg/kg once every three days. Gefitinib (100mg/kg, MCE, #HY-50895) were administered to mice by gavage every day. Anti-Mouse PD-1 antibody (200ug per mouse, MCE, #HY-P99144) were intraperitoneally injected once every three days. Mice accepted PBS were the control group. The medication is blindly administered by a professional mice keeper. All groups of mice were euthanized and the whole intestine tract was harvested after 21 days of treatment.

Tumor volumes (major diameter * minor diameter^2/2) and weights were measured. The surgery for mice were performed by the same one researcher, while the cells was blindly prepared by another researcher. To further reduce bias, the mice that needed to be compared accepted surgery on the same day and were injected with the same batch of cells.

Depletion of macrophages in mice

Macrophages were pharmacologically depleted using clodronate liposome (5 mg/mL, 40337ES10; Yeasen, Shanghai, China).[44] Briefly, 200μL PBS (control) or clodronate liposome were intraperitoneally injected into 5-week-old male C57BL/6 mice 3 days before undergoing appendectomy. And mice accepted injection of clodronate liposome (100ul/per) or PBS twice every week during experiment to keep the depletion of macrophages. Depletion of macrophages were analyzed by flow cytometry.

Multicolor flow cytometric analysis

The tumor tissues from Orthotopic mouse models were excised for immune profiling and were dissected into small pieces and digested with 1% bovine serum albumin (BSA) containing 0.5mg/ml collagenase IV (Solarbio, China) and 0.25mg/ml DNase (Roche) for 45 minutes at 37°C on a shaking platform. The cell suspension was then filtered through a 70-μm cell strainer and centrifuged at 500 g for 5 minutes. The cell pellets were resuspended in 1% BSA for surface marker staining. Flow cytometry was performed on Agilent NovoCyte Flow Cytometer (BD Biosciences). Data were analyzed by NovoExpress 1.6.0. Antibodies used in this study are listed in key resources table. Gating strategy is illustrated in Figure S6.

Characterization of M1 macrophage associated with OS in the cancer Genome Atlas (TCGA) cohort

The RNA expression profiles and clinical information for CRC were downloaded from the TCGA database (https://portal.gdc.cancer.gov/repository), which included 474 cases of CRC. We excluded CRC patients from the TCGA dataset based on the following criteria: (1) Age < 18 years on the index day; (2) patients with other malignancies; (3) patients who received radiotherapy and chemotherapy prior to surgery. Finally, 326 patients with CRC were selected for our study (Figure S7). M1 macrophage cell infiltration was analyzed using CIBERSORT. High M1 macrophage infiltration (n=163) was distinguished based on the median value and the clinical characteristics of the study population in TCGA were shown in Table S13. Kaplan Meier prognosis analysis was performed to assess the association between the density of M1 macrophages and the OS of patients. This study adheres to the publication guidelines set forth by TCGA.

Compare the abundance of candidate bacteria between APD-CRC and CON-CRC by qPCR

Bacteria DNA was extracted from the cohort of 12 cancer tissues and paired normal tissue from CRC patients with appendectomy and 24 paired tissues from control CRC (matched 1:2 by age, sex, location, BMI) using the QIAamp DNA Mini kit (Qiagen) according to the manufacturer's instruction. Abundances of candidate bacteria were estimated in samples using SYBRGreen quantitative PCR (qPCR). Primer sequences are in Table S14. The abundance of the microbial markers was calculated as a relative unit normalized to the total bacteria of that sample using the $2^{-\Delta Ct}$ method (where ΔCt=the average Ct value of each target - the average Ct value of total bacteria).[45]

Analysis for prediction of drug sensitivity

The NTP-based classification was performed in TCGA to evaluate the association of a set of gene signatures about drug sensitivity with the density of M1 macrophage cells by R program.[46] The lists of gene signatures about drug sensitivity are showed in Table S15.[47] The threshold selected for the significance of each case was Benjamini–Hochberg-corrected FDR < 0.2. The association of the FOLFIRI response signature and FOLFOX response signature with the density of M1 macrophage cells was further determined by the same method applied in Sumaiyah K. Rehman's paper. The expression value (z-score) was multiplied by -1 if the genes were from resistance signatures of chemotherapy regimens, while the value of genes from sensitivity signatures was kept unchanged. For each sample, the signature score was then computed as the mean of all genes.

In this study, T cell–inflamed gene expression profile (GEP) scores and mutation signature analysis were calculated to predict sensitiveness of APD-CRC characterized by low density of M1 macrophages in TCGA datasets to immunotherapy. GEP scores were calculated as a weighted sum of normalized expression values for the 18 genes, which was composed of 18 inflammatory genes related to antigen presentation, chemokine expression, cytolytic activity, and adaptive immune resistance, including CCL5, CD27, CD274 (PD-L1), CD276 (B7-H3), CD8A, CMKLR1, CXCL9, CXCR6, HLA-DQA1, HLA-DRB1, HLA-E, IDO1, LAG3, NKG7, PDCD1LG2 (PDL2), PSMB10, STAT1, and TIGIT.[48] The TCGA database was utilized to generate the mutation annotation format (MAF) using the "maftools" R package. Furthermore, we calculated the tumor mutational burden (TMB) score for both cohorts of colorectal cancer patients.[49]

Enriched pathways of CRC tissue with low density of M1 macrophage cells

We performed Pearson correlation coefficient analysis to find to signaling pathways correlated with the density of M1 macrophage cells based on RNA-seq data of mice CRC tissue. GSVA was performed to validate the relationship between significant signaling pathways and the density of M1 macrophage cells in the TCGA-CRC cohort.

QUANTIFICATION AND STATISTICAL ANALYSIS

Two-tailed Students' t test, Fisher's exact test, χ^2 test, and Wilcoxon test was performed respectively using the R program (v.3.4.1). In all these tests, statistical significance was set at 0.05. In the NTP algorithm, the results were regarded as significant if the Benjamini–Hochberg FDR was <0.2. For animal experiment, the data used for comparison were collected from the same batch of mice.